JACS
JOURNAL OF THE AMERICAN CHEMICAL SOCIETY
Article
pubs.acs.org/JACS

Investigating the Reactivity of Radical Cations: Experimental and Computational Insights into the Reactions of Radical Cations with Alcohol and *p*-Toluene Sulfonamide Nucleophiles

John M. Campbell, Hai-Chao Xu, and Kevin D. Moeller*

Washington University in Saint Louis, Saint Louis, Missouri 63130, United States

Supporting Information

ABSTRACT: The reactivity of electrochemically generated radical cations toward alcohol and *p*-toluene sulfonamide nucleophiles was directly investigated through competition experiments. Alcohol-trapping of the radical cation is the kinetically favored pathway and is reversible. Trapping with the sulfonamide leads to the thermodynamic product. Both reaction pathways were investigated computationally with density functional theory (UB3LYP/6-31G(d)) calculations.

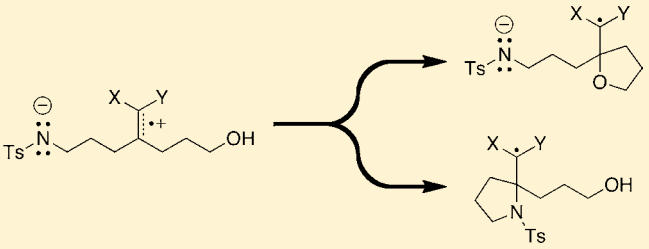

INTRODUCTION

Radical cations are important intermediates in organic chemistry and may be employed to initiate and accomplish a variety of reactions and transformations.[1−6] Our work has focused on the chemistry of radical cations generated by electrochemical oxidation of electron-rich double bonds. The reactions are of synthetic interest because they reverse the polarity of enolate equivalents in a manner that allows them to function as an electrophile.[7,8] The reactions are easily implemented[9] and general in their application.[10] However, an accurate mechanistic and kinetic understanding of these reactions can be difficult to achieve. Newcomb and co-workers nicely explored the chemistry of enol ether radical cations and were able to establish reaction rates.[11] We seek to further investigate the chemoselectivity of radical cation reactions and explore the reactivity of radical cations formed from a variety of electron-rich olefins.

To address these questions, a competition experiment was designed so that the relative reactivity of olefin-based radical cations toward various intramolecular nucleophiles can be directly investigated. As shown in Scheme 1, the plan calls for an electron-rich olefin to be tethered to two different nucleophiles. Upon oxidation of **1**, the radical cation intermediate **2** can be trapped by either nucleophile. The ratio of the products ultimately formed (**3** and **4**) will then yield information on the relative selectivity of the radical cation for the two nucleophiles.

Initial efforts along these lines have focused on substrates with an alcohol and a *p*-toluene sulfonamide nucleophile (**5**, Scheme 2). The studies were motivated by the observation that oxidative cyclizations between electron-rich olefins and sulfonamide nucleophiles benefited greatly from the use of basic reaction conditions.[12,13] The base deprotonated the sulfonamide prior to the electrolysis, a situation that led to questions about the mechanism of the cyclization. Did the addition of base aid the cyclization by enhancing the nucleophilic addition of the sulfonamide to the radical cation

Scheme 1. General Design of a Competition Study[a]

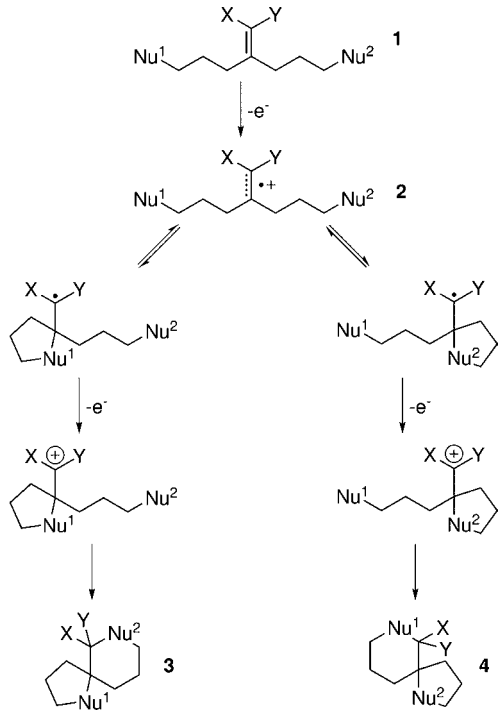

[a]The products obtained (**3** and **4**) yield information on the relative selectivity of the radical cation **2** for the two different nucleophiles (X,Y = electron donating).

Received: July 18, 2012
Published: October 13, 2012

   dx.doi.org/10.1021/ja307046j | J. Am. Chem. Soc. 2012, 134, 18338−18344

Scheme 2. Substrate for the Competition Experiment Presented in This Article[a]

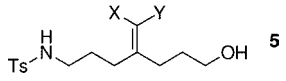

[a]X,Y = electron donating.

Scheme 3. Mechanism for Sulfonamide-Cyclization May Proceed through Either 7 or 8[a]

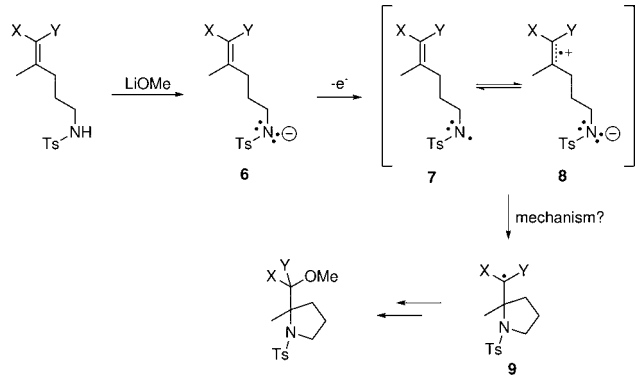

[a]X,Y = electron donating.

(intermediate **8**, Scheme 3), or did it change the mechanism of the reaction so that the cyclization resulted from the addition of a nitrogen radical to the olefin (intermediate **7**, Scheme 3)? The two mechanisms are potentially related by a fast intramolecular electron-transfer reaction between the two key intermediates **7** and **8**. Both reaction pathways lead to intermediate **9**.

The alcohol was selected as a competitor for the sulfonamide because it is known to efficiently trap radical cations.[14] Furthermore, unlike many alternative trapping groups, its use does not add an additional stereocenter to the cyclized products.

A second goal of this research was to determine how substituents on the double bond (X and Y in **5**) alter the selectivity of the reaction. Within the context of intramolecular anodic olefin coupling reactions, it has been observed that the olefin substituents can have significant effects on the overall success and chemoselectivity of a cyclization.[15] In this study, we explore the use of enol ethers, ketene dithioacetals, and vinyl sulfides.[16]

In the initial study,[16] the mechanism of the sulfonamide-cyclization was probed by examining the effect of solvent polarity on the oxidation of **5**. The experiments confirmed that the intramolecular electron transfer shown in Scheme 3 did happen. In addition, cyclization with the sulfonamide nucleophile in **5** benefited from the use of nonpolar reaction conditions, while the amount of alcohol-trapping increased with the use of a more polar medium. These observations were consistent with a kinetically controlled reaction that was governed by the Curtin–Hammett principle.

Recent computational studies suggest that this picture of the mechanism is overly simplistic, a conclusion that is supported by the effect that both temperature and current density have on the reactions. We report here that the alcohol-trapping pathway that results from the oxidation of **5** leads to the kinetic product. With the reaction conditions used previously, this reaction is reversible. The sulfonamide-based cyclization leads to the formation of the thermodynamic product.

RESULTS AND DISCUSSION

Our initial understanding of the reaction originating from the oxidation of **5** is illustrated in Scheme 4. We postulated that if the reaction was kinetically controlled, it would be governed by

Scheme 4. An Initial Guess at the Energy Profile for This Competition Experiment

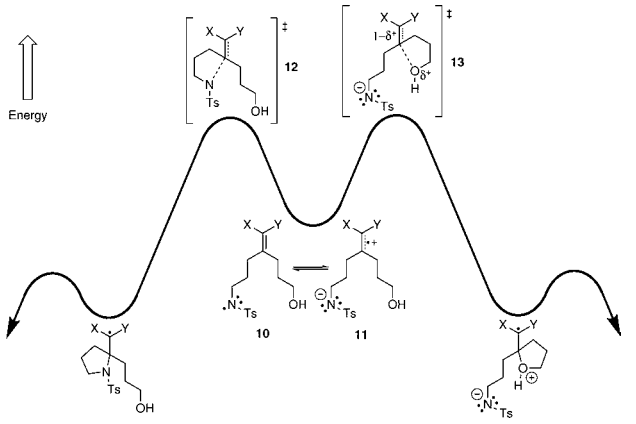

the nature of the initial cyclization of **10** and/or **11**, that is, the relative energies of the sulfonamide-cyclization and the alcohol-trapping transition states, **12** and **13**, respectively. This hypothesis was consistent with an application of the Curtin–Hammett principle, an approach that had served us well in the past.[17] We were eager to see whether or not the Curtin–Hammett principle would apply in this case.

It was noted that the sulfonamide-cyclization pathway proceeded through a transition state (**12**) that was likely to exhibit very little charge separation, especially in comparison to the zwitterionic transition state of the alcohol-trapping pathway (**13**). With this in mind, it appeared possible to select for sulfonamide-cyclization with the use of a nonpolar reaction medium. Such a medium is achieved through the choice of solvent and electrolyte.

Solvent Experiments. Tables 1–3 show the results of several solvent polarity studies. In all cases, the use of 100% methanol as a solvent and lithium perchlorate as an electrolyte produced products arising from both sulfonamide-cyclization and alcohol-trapping. Upon the addition of tetrahydrofuran as a cosolvent, up to 30% MeOH/THF, an increase in sulfonamide-cyclization relative to alcohol-trapping was observed. Furthermore, using tetraethylammonium tosylate instead of lithium perchlorate as the electrolyte also served to decrease the polarity of the reaction medium and led to an increase in sulfonamide-cyclization. Selectivity for alcohol-trapping was most successfully achieved by substituting 2,6-lutidine for lithium methoxide as a base, thereby avoiding deprotonation of the sulfonamide.

In the case of the enol ether-derived radical cation, the yield of alcohol-trapping products was low even with the use of 2,6-lutidine as the base. The low yield appeared to be due to the instability of **15c** and **15d**. No such problem arose following the oxidation of the ketene dithioacetal and vinyl sulfide substrates.

In the case of the vinyl sulfide (Table 3), electrolysis of initially synthesized substrates led to only sulfonamide-cyclization products in all cases. Thus, for this particular

dx.doi.org/10.1021/ja307046j | J. Am. Chem. Soc. 2012, 134, 18338–18344

Table 1. Results of Solvent Polarity Experiments for an Enol Ether Substrate

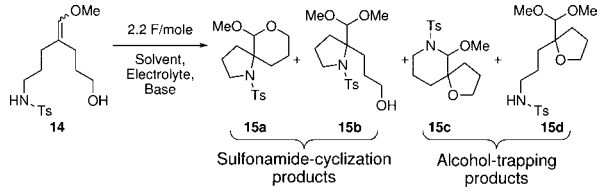

solvent (electrolyte, base)	% yield 15a + 15b	15c + 15d
100% MeOH ($LiClO_4$, LiOMe)	48 (36 + 12)	10 (0 + 10)
60% MeOH/THF ($LiClO_4$, LiOMe)	85 (66 + 19)	0
30% MeOH/THF ($LiClO_4$, LiOMe)	79 (62 + 17)	0
100% MeOH (Et_4NOTs, LiOMe)	83 (75 + 8)	0
60% MeOH/THF (Et_4NOTs, LiOMe)	82 (66 + 16)	0
30% MeOH/THF (Et_4NOTs, LiOMe)	91 (71 + 20)	0
30% MeOH/THF[a] ($LiClO_4$)	0	20 (0 + 20)
30% MeOH/THF[a] (Et_4NOTs)	0	27 (0 + 27)

[a]2,6-Lutidine was used as a base.

Table 2. Results of Solvent Polarity Experiments for a Ketene Dithioacetal Substrate

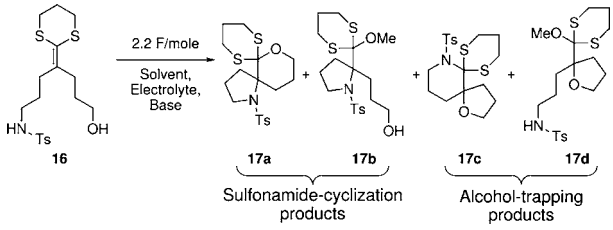

solvent (electrolyte, base)	% yield 17a + 17b	17c + 17d
100% MeOH ($LiClO_4$, LiOMe)	50 (40 + 10)	27 (27 + 0)
60% MeOH/THF ($LiClO_4$, LiOMe)	75 (62 + 13)	16 (16 + 0)
30% MeOH/THF ($LiClO_4$, LiOMe)	83 (71 + 12)	3 (3 + 0)
100% MeOH (Et_4NOTs, LiOMe)	58 (48 + 10)	20 (20 + 0)
60% MeOH/THF (Et_4NOTs, LiOMe)	76 (66 + 16)	6 (6 + 0)
30% MeOH/THF (Et_4NOTs, LiOMe)	87 (70 + 17)	0
30% MeOH/THF[a] ($LiClO_4$)	0	87 (72 + 15)
30% MeOH/THF[a] (Et_4NOTs)	0	56 (39 + 17)

[a]2,6-Lutidine was used as a base.

substrate, we chose to extend the tether connecting the sulfonamide to the olefin by one methylene unit. This slowed the sulfonamide-cyclization and allowed alcohol-trapping to compete, although it also led to lower overall yields and lower current efficiency due to side reactions associated with sulfonamide-cyclizations forming six-membered rings.[13]

All three electrolysis substrates behaved according to the same general trend. Nonpolar conditions favored sulfonamide-cyclization, while polar conditions favored alcohol-trapping. Differences in selectivity between the three substrates were attributed to the olefin substituents.

Oxidation Potentials. To gain further insight into the mechanism of sulfonamide-cyclization, the oxidation potentials of the functional groups involved in the cyclization were investigated. Interestingly, the deprotonated sulfonamide exhibited an oxidation potential lower than either the enol ether, the ketene dithioacetal, or the vinyl sulfide ($E_{p/2}$ = 0.9 V vs Ag/AgCl, Table 4). The potentials for the olefins were measured without the addition of lithium methoxide (conditions A). It is worth noting that potentials measured for the substrates in the presence of lithium methoxide (conditions B) were lower than that of the sulfonamide anion (entry 4B). This finding is consistent with a cyclization that occurs at or near the electrode surface.[18]

Before interpreting the oxidation potentials, it is important to recognize that the preparative electrolysis experiments were run under constant current conditions. This means that the voltage across the cell was varied dynamically to maintain a preset current. In such experiments, the potential at the working electrode adjusts automatically to match the functional group with the lowest oxidation potential. Hence, given the data in Table 4, the preparative reactions led to initial oxidation of the sulfonamide anion and the formation of an olefin/nitrogen radical pair. This is interesting because the alcohol in our competition experiments cyclized competitively with the sulfonamide, a transformation that requires formation of the radical cation at the olefin. Clearly, an intramolecular electron transfer between the olefin and the sulfonamide anion does occur.

Table 3. Results of Solvent Polarity Experiments for a Vinyl Sulfide Substrate[a]

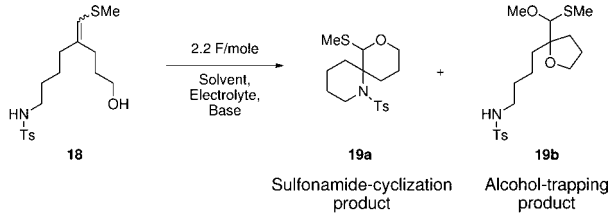

solvent (electrolyte, base)	% yield 19a	19b
100% MeOH[b] ($LiClO_4$, LiOMe)	28	19
60% MeOH/THF[b] ($LiClO_4$, LiOMe)	25	16
30% MeOH/THF[b] ($LiClO_4$, LiOMe)	29	9
100% MeOH[c] (Et_4NOTs, LiOMe)	54	0
60% MeOH/THF[c] (Et_4NOTs, LiOMe)	45	0
30% MeOH/THF[c] (Et_4NOTs, LiOMe)	34	0
30% MeOH/THF[d] ($LiClO_4$)	0	44
30% MeOH/THF[d] (Et_4NOTs)	0	79

[a]In this case, the sulfonamide tether was extended by one methylene unit. [b]3.0 F/mol passed during electrolysis. [c]4.0 F/mol passed during electrolysis. [d]2,6-Lutidine was used as a base.

Table 4. Half-Wave Oxidation Potentials ($E_{p/2}$) for Various Functional Groups

Entry	Substrate	Conditions[a]	$E_{p/2}$ (V)
1	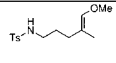	A	1.18
		B	0.78
2	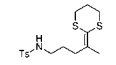	A	0.98
		B	0.69
3	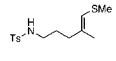	A	1.08
		B	0.77
4	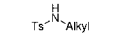	A	>1.8[b]
		B	0.9

[a]A: Carbon anode, platinum cathode, Ag/AgCl reference electrode, scan rate 50 mV/s, 0.1 M Et_4NOTs, substrate concentration of 0.025 M in methanol. B: 0.6 equiv of LiOMe was added. [b]Oxidation potential exceeded that of the solvent.

dx.doi.org/10.1021/ja307046j | J. Am. Chem. Soc. 2012, 134, 18338−18344

Computational Results.[19] Pushing for a deeper understanding of the mechanisms of sulfonamide-cyclization and alcohol-trapping, we turned to a computational approach.

Density functional theory (DFT) has been utilized by others[20−25] to investigate the chemistry of radical cations due to its low computational cost and ability to avoid problems of spin contamination, a serious consideration when modeling open-shell molecules.[26] However, the limitations of DFT, including its tendency to underestimate dissociation barriers[27] and to unduly delocalize spin and charge,[22,28] are well documented. Hence, all calculations reported herein are presented as a supplement to the experimental data. We elected to use the unrestricted B3LYP functional due to its successful application to other radical cation systems. Recently, other functionals have enjoyed successful application to radical cation systems, especially the M06 family of functionals.[29]

Transition structures for sulfonamide-cyclization with an enol ether, a ketene dithioacetal, and a vinyl sulfide were located using DFT (UB3LYP/6-31G(d)) and are depicted in Figures 1−3. The alcohol tether was excluded from the calculation to save computation time. Each transition structure exhibited only one vibration with an imaginary frequency. The length of the forming nitrogen−carbon bond was between 2.07 and 2.21 Å, depending on the olefin substituents.

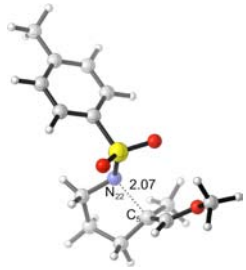

Figure 1. Transition structure for the coupling of a sulfonamide to an enol ether.

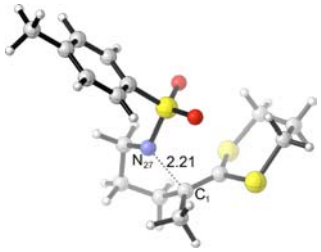

Figure 2. Transition structure for the coupling of a sulfonamide to a ketene dithioacetal.

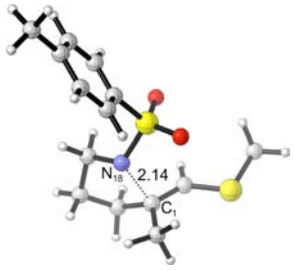

Figure 3. Transition structure for the coupling of a sulfonamide to a vinyl sulfide.

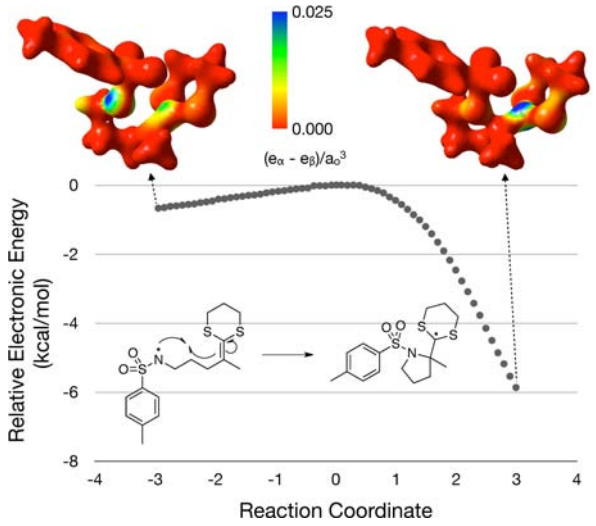

Figure 4. Intrinsic reaction coordinate (IRC) around the transition structure for the coupling of a sulfonamide with a ketene dithioacetal. The color maps shown represent the unpaired electron density (expressed in units of unpaired electrons per cubic bohr $(e_\alpha - e_\beta)/a_o^3$) mapped onto the total electron density surface.

The intrinsic reaction coordinate (IRC) around each transition structure was then computed. In all sulfonamide-cyclizations, the unpaired electron spin in the intermediates leading from the reactant to the transition structure was primarily localized at the nitrogen of the sulfonamide. For a representative example, see Figure 4. These results indicated that sulfonamide-cyclization is best described as a radical-like cyclization. This finding contradicts the conclusions reported from our earlier investigation of this competition experiment[16] in which we postulated that the reaction involved an olefin-localized radical cation and an anionic sulfonamide nucleophile.

To quantify the energetics associated with sulfonamide-cyclization, energies of activation and net changes in energy were calculated and are presented in Table 5. Our conclusions

Table 5. Calculated Activation Energies (E_{act}) and Net Changes in Energy (ΔE) Given in Terms of Electronic Energy (E_{SCF}) and Gibbs Free Energy (G)

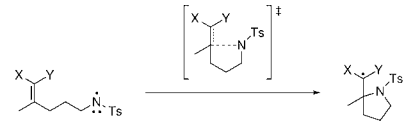

	E_{act} (kcal/mol)		ΔE (kcal/mol)	
	$\Delta E^{\ddagger}_{SCF}$	$\Delta G^{\ddagger}$	ΔE_{SCF}	ΔG
	1.8	3.6	-5.2	-2.3
	1.2	3.1	-11.1	-9.5
	2.1	3.7	-7.1	-5.1

from these data are that sulfonamide-cyclization is exothermic and has a low-to-modest energy of activation that is on the order of a few kcal/mol depending on the identity of the olefin substituents.

Similar attempts to explore the alcohol-trapping pathway computationally were not as successful. Unable to find a transition structure, we submitted the simplified product of an

dx.doi.org/10.1021/ja307046j | J. Am. Chem. Soc. 2012, 134, 18338−18344

Scheme 5. Distonic Radical Cation 21 Not at a Local Energy Minima[a]

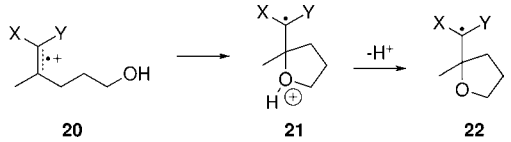

[a]No transition structure for the cyclization or the deprotonation could be found.

alcohol-trapping cyclization to Gaussian for geometric optimization (**21**, Scheme 5). However, this structure was not at an energy minimum. Instead, the optimized geometry was that of the starting material (**20**), with the unpaired electron spin distributed over both carbons of the olefin. Hence, it was postulated that a deprotonation of the alcohol occurs in the transition state of the cyclization, leading directly to **22**.

Such a hypothesis is not without precedent. Zipse reported a computational investigation of the reaction of water and ethylene radical cation.[30] It was found that the formation of a distonic radical cation had no barrier, and that the resultant product was highly acidic. Furthermore, Okazaki and coworkers published a kinetics study of reactions of alcohols with 9,10-diphenylanthracene radical cations, concluding that deprotonation of the alcohol was the rate-determining step of the reaction.[31] More recently, Arnold and Newcomb have both proposed that a deprotonation is involved in the alcohol-trapping of olefin-based radical cations.[5,32]

Despite this mechanistic insight, a transition structure for alcohol-trapping could not be found, and the search for one was abandoned. Furthermore, attempts to quantify the energetics involved in alcohol-trapping were also unsuccessful in that the calculation results were not consistent with experiment. Alcohol-trapping involves the neutralization of a charged species and a deprotonation, both of which are likely to occur at or near the electrode, that is, within the electrical double layer and surrounded by electrolyte. It is likely that limitations of the commonly available solvation models prohibit an accurate calculation of the relevant species.

While sulfonamide-cyclizations also occur at or near the electrode surface, they are entirely intramolecular, involve no formal charges, and are more isodesmic in nature. For these reasons, we believe that a computational investigation of sulfonamide-cyclization is less prone to error.

At this point, we turned to an experimental approach to explore the energetics of alcohol-trapping relative to sulfonamide-cyclization. With the energetics of sulfonamide-cyclization in hand, we were eager to see which of the two pathways was the kinetically favored one. Thus far, the competition experiments appeared to indicate that sulfonamide-cyclization was kinetically favored under most reaction conditions (see Tables 1–3). However, if indeed the barrier to alcohol-trapping involved only an intramolecular electron transfer and a deprotonation, how high could the alcohol-trapping barrier be relative to the energetics presented in Table 5? We decided to begin by exploring the effects of reaction temperature on our competition experiments.

Temperature Experiments. The electrolysis reactions were repeated, varying the reaction temperature from as high as 45 °C to as low as −42 °C. As shown in Tables 6–8, lower temperatures led to an increase in the yield of alcohol-trapping products relative to sulfonamide-cyclization products. As

Table 6. Results of Temperature Experiments for an Enol Ether Substrate

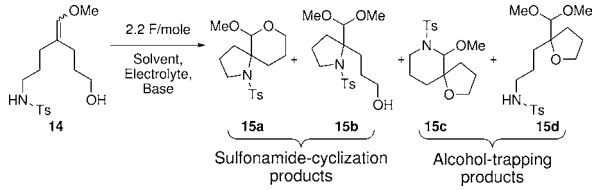

	% yield	
temp (°C)	**15a + 15b**	**15c + 15d**
45	65 (9 + 56)	0
25	46 (6 + 40)	7 (0 + 7)
0	3 (3 + 0)	37 (0 + 37)
−15	2 (2 + 0)	33 (0 + 33)
−42	4 (4 + 0)	33 (0 + 33)

Table 7. Results of Temperature Experiments for a Ketene Dithioacetal Substrate

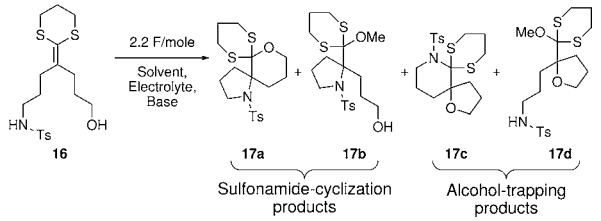

	% yield	
temp[a] (°C)	**17a + 17b**	**17c + 17d**
45	71 (62 + 9)	26 (24 + 2)
25	50 (40 + 10)	27 (27 + 0)
0	31 (31 + 0)	38 (34 + 4)
−23	18 (18 + 0)	37 (33 + 4)
−42	9 (9 + 0)	15 (15 + 0)

[a]The starting material became insoluble at lower temperatures.

Table 8. Results of Temperature Experiments for a Vinyl Sulfide Substrate

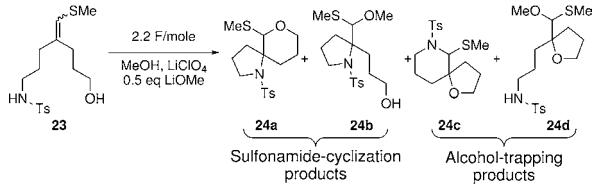

	% yield	
temp (°C)	**24a + 24b**	**24c + 24d**
25	82 (30 + 52)	1–3 (0 + 1–3)
0	53 (28 + 25)	21 (0 + 21)
−23	32 (13 + 19)	38 (3 + 35)
−42	28 (6 + 22)	46 (4 + 42)

temperatures are lowered, alcohol-trapping eventually becomes the major pathway. In the case of the enol ether (Table 6), isolation of the alcohol-trapping products remains problematic, and as a result the yields reported are low. In the case of the ketene dithioacetal (Table 7), the starting material becomes insoluble in the solvent at low temperatures, leading to lower overall yields at lower temperatures.

The fact that lower temperatures lead to an increase in alcohol-trapping products indicates that the enthalpic energy

dx.doi.org/10.1021/ja307046j | J. Am. Chem. Soc. 2012, 134, 18338–18344

barrier ($\Delta H^{\ddagger}$) to alcohol-trapping is lower than that of sulfonamide-cyclization. Yet, at high temperatures, sulfonamide-cyclization becomes the major product. There are two possible explanations for this. First, the entropic energy barrier ($\Delta S^{\ddagger}$) may be smaller for sulfonamide-cyclization. If this were the case, then alcohol-trapping would be kinetically favored at lower temperatures and sulfonamide-cyclization kinetically favored at higher temperatures. This seemed very plausible, given the evidence for a deprotonation in the alcohol-trapping transition state.

The second possibility is that the reactions at higher temperatures are under thermodynamic control. This would mean that higher temperatures allow for equilibration to the thermodynamic product, while lower temperatures select for the formation of the kinetic product. For this to be the case, alcohol-trapping of the radical cation would need to be reversible.

Current Density Experiments. What was needed to distinguish the two mechanistic possibilities was a method that would alter the reversibility of the cyclization without changing the temperature (and hence $T\Delta S^{\ddagger}$) of the reaction. In an electrolysis reaction, this can be accomplished by varying the current density. Consider the working model for the cyclizations illustrated in Scheme 6.

Scheme 6. Kinetics of the Cyclization of a Radical Cation with a Nucleophile

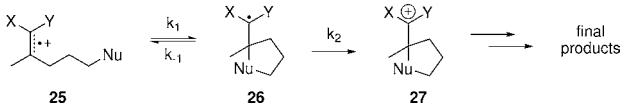

In this scenario, the reversibility of the cyclization of **25** (whose forward and reverse rates are indicated by k_1 and k_{-1}, respectively) is determined by k_2. When $k_2 < k_{-1}$, the cyclization reaction is under thermodynamic control, and the cyclization that leads to the lowest-energy intermediate will give rise to the major product. When $k_2 \approx k_{-1}$, the cyclization is governed by steady-state kinetics. When $k_2 > k_{-1}$, the cyclization reaction is under kinetic control, and it is the cyclization with the lowest energy of activation that leads to the major product of the reaction. So, if we can accelerate the second oxidation (make k_2 larger), then a thermodynamically controlled process can be converted to a kinetically controlled one. One of the advantages of anodic oxidation is that the rate of oxidation can be directly controlled. By increasing or decreasing the flow of current, we can alter the rate of electron transfer and hence the rate at which both the substrate and the radical **26** are oxidized. A fast rate of oxidation can be used to select the kinetic cyclization.

Applying this method to the oxidation of substrate **5** led to the results reported in Table 9. For all three substrates, sulfonamide-cyclization was favored when the current was set to 6 mA. However, when the current was increased to 46 mA, alcohol-trapping was favored. These results showed that alcohol-trapping leads to the kinetic product of the electrolysis reactions. Furthermore, it demonstrated that alcohol-trapping of the radical cation is reversible. This is evidenced by the fact that if the current is low enough, the intermediates will equilibrate to the thermodynamically favored intermediate product.

Table 9. Results of Current Experiments for Anodic Coupling Reactions

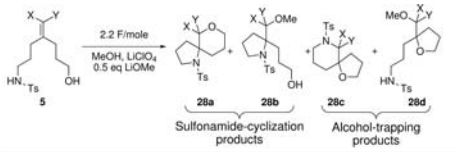

	Current (mA)	% Yield (**28a** + **28b**)	% Yield (**28c** + **28d**)
	6	46 (6 + 40)	7 (0 + 7)
	46	5 (0 + 5)	43 (0 + 43)
	6	50 (40 + 10)	27 (27 + 0)
	46	25 (21 + 4)	38 (35 + 3)
	6[a]	53 (28 + 25)	21 (0 + 21)
	46[a]	18 (10 + 8)	48 (7 + 41)

[a]Reaction temperature kept at 0 °C.

CONCLUSION

Our current understanding of the competition experiment reported herein, based upon our experimental and computational investigations, is illustrated in Scheme 7. Our experimental results, taken all together, indicate that the reaction is not under Curtin–Hammett control as we previously reported.[16] Instead, it is a competition between the kinetic pathway and the thermodynamic one.

Scheme 7. Revised Understanding of the Energy Profile for This Competition Experiment

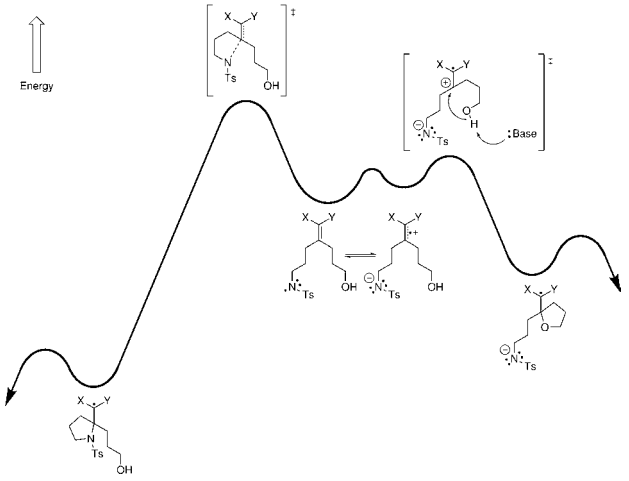

The anodic coupling of a sulfonamide to an electron-rich olefin under basic conditions exhibited a radical-like mechanism, with the initial oxidation occurring at the deprotonated sulfonamide. However, an intramolecular electron transfer occurs that affords an olefinic radical cation. This radical cation can be trapped by a competing alcohol nucleophile. When in direct competition with alcohol-trapping, sulfonamide-cyclization was found to afford the thermodynamically favored product and may be enhanced with nonpolar reaction conditions, elevated temperatures, and low current. Alcohol-trapping of the radical cation was found to be facile, reversible, and afforded the kinetically favored product. Alcohol-trapping may be promoted with polar reaction conditions, low temperatures, and high current.

dx.doi.org/10.1021/ja307046j | J. Am. Chem. Soc. 2012, 134, 18338–18344

These conclusions are consistent with earlier observations of radical cation/alcohol-trapping reactions and may well have broad implications for a variety of radical cation-induced cyclizations. Effort to extend these findings to additional cyclizations is continuing with the use of new competition substrates.

■ ASSOCIATED CONTENT

Supporting Information

A general procedure for the electrolysis reaction, procedures for the synthesis of electrolysis substrates, characterization of electrolysis substrates, and a description of the computational methods for calculating optimized geometries, transition structures, and intrinsic reaction coordinates. This material is available free of charge via the Internet at http://pubs.acs.org.

■ AUTHOR INFORMATION

Corresponding Author

moeller@wuchem.edu

Notes

The authors declare no competing financial interest.

■ ACKNOWLEDGMENTS

This work is supported by the National Science Foundation, grant CHE-0809142. The Washington University Computational Chemistry Facility was constructed with support from the National Science Foundation, grant CHE-0443501.

■ REFERENCES

(1) Schmittel, M.; Burghart, A. *Angew. Chem., Int. Ed. Engl.* **1997**, *36*, 2550−2589.

(2) (a) Jang, H.-Y.; Hong, J.-B.; MacMillan, D. W. C. *J. Am. Chem. Soc.* **2007**, *129*, 7004−7005. (b) Beeson, T. D.; Mastracchio, A.; Hong, J.-B.; Ashton, K.; MacMillan, D. W. C. *Science* **2007**, *27*, 582−585. (c) J. J. D., III; Conrad, J. C.; MacMillan, D. W. C.; R. A. F., II. *Angew. Chem., Int. Ed.* **2010**, *49*, 6106−6110.

(3) (a) Liu, L.; Floreancig, P. E. *Org. Lett.* **2009**, *11*, 3152−3155. (b) Liu, L.; Floreancig, P. E. *Angew. Chem., Int. Ed.* **2010**, *49*, 5894−5897. (c) Tu, W.; Liu, L.; Floreancig, P. E. *Angew. Chem., Int. Ed.* **2008**, *47*, 41844187. (d) Green, M. E.; Rech, J. C.; Floreancig, P. E. *Angew. Chem., Int. Ed.* **2008**, *47*, 7317−7320. (e) Jung, H. H.; J. R. S., II; Floreancig, P. E. *Angew. Chem., Int. Ed.* **2007**, *46*, 8464−8467. (f) Floreancig, P. E. *Synlett* **2007**, 191−203.

(4) (a) Horner, J. H.; Newcomb, M. *J. Org. Chem.* **2007**, *72*, 1609−1616. (b) Horner, J. H.; Lal, M.; Newcomb, M. *Org. Lett.* **2006**, *8*, 5497−5500. (c) Bagnol, L.; Horner, J. H.; Newcomb, M. *Org. Lett.* **2003**, *5*, 5055−5058.

(5) Horner, J. H.; Bagnol, L.; Newcomb, M. *J. Am. Chem. Soc.* **2004**, *126*, 14979−14987.

(6) (a) Crich, D.; Sirai, M.; Brebion, F.; Rumthao, S. *Tetrahedron* **2006**, *62*, 6501−6518. (b) Crich, D.; Sirai, M.; Brebion, F.; Rumthao, S. *Org. Lett.* **2003**, *5*, 3767−3769.

(7) Little, R. D.; Moeller, K. D. *Electrochem. Soc. Interface* **2002**, *11*, 36−42.

(8) Tang, F.; Chen, C.; Moeller, K. D. *Synthesis* **2007**, 3411−3420.

(9) Frey, D. A.; Wu, N.; Moeller, K. D. *Tetrahedron Lett.* **1996**, *37*, 8317−8320.

(10) Moeller, K. D. *Synlett* **2009**, *8*, 1208−1218.

(11) Horner, J. H.; Taxil, E.; Newcomb, M. *J. Am. Chem. Soc.* **2002**, *124*, 5402−5410.

(12) Xu, H.-C.; Moeller, K. D. *J. Am. Chem. Soc.* **2008**, *130*, 13542−13543.

(13) Xu, H.-C.; Moeller, K. D. *J. Am. Chem. Soc.* **2010**, *132*, 2839−2844.

(14) Xu, G.; Moeller, K. D. *Org. Lett.* **2010**, *12*, 2590−2593 and references therein.

(15) Tang, F.; Moeller, K. D. *Tetrahedron* **2009**, *65*, 10863−10875.

(16) For a preliminary account of this work, see: Xu, H.-C.; Moeller, K. D. *Org. Lett.* **2010**, *12*, 1720−1723.

(17) Redden, A.; Moeller, K. D. *Org. Lett.* **2011**, *13*, 1678−1681.

(18) Xu, H.-C.; Moeller, K. D. *Angew. Chem., Int. Ed.* **2010**, *49*, 8004−8007.

(19) Density functional theory (DFT) was used to calculate optimized geometries, find transition structures, and compute intrinsic reaction coordinate pathways using the unrestricted B3LYP functional, a 6-31G(d) basis set, and the PCM methanol solvation model. Initial molecular geometries were built and optimized using semi-emperical methods (AM1) in Spartan (*Spartan '10*; Wavefunction, Inc.: Irvine, CA). These geometries were then imported into the Gaussian 03 suite of programs (Frisch, M. J.; et al. *Gaussian 03*, revision C.02; Gaussian, Inc.: Wallingford, CT, 2004) for all subsequent calculations. Calculations were performed at the Washington University in Saint Louis Computational Chemistry Facility. Images of transition structures were generated using CYLview (Legault, C. Y. *CYLview*, 1.0b; Université de Sherbrooke, 2009 (http://www.cylview.org)).

(20) (a) Wiest, O. *J. Am. Chem. Soc.* **1997**, *119*, 5713−5719. (b) Haberl, U.; Wiest, O.; Steckhan, E. *J. Am. Chem. Soc.* **1999**, *121*, 6730−6736. (c) Swinarski, D. J.; Wiest, O. *J. Org. Chem.* **2000**, *65*, 6708−6714. (d) Radosevich, A. T.; Wiest, O. *J. Org. Chem.* **2001**, *66*, 5808−5813. (e) Oxgaard, J.; Wiest, O. *J. Phys. Chem. A* **2002**, *106*, 3967−3974. (f) Donoghue, P. J.; Wiest, O. *Chem.-Eur. J.* **2006**, *12*, 7018−7026. (g) Valley, N. A.; Wiest, O. *J. Org. Chem.* **2007**, *72*, 559−566.

(21) (a) Fry, A. J. *Tetrahedron* **2008**, *64*, 2101−2103. (b) Wu, X.; Davis, A. P.; Lambert, P. C.; Steffen, L. K.; Toy, O.; Fry, A. J. *Tetrahedron* **2009**, *65*, 2408−2414.

(22) Sodupe, M.; Rodríguez-Santiago, J. B. L.; Baerends, E. J. *J. Phys. Chem. A* **1999**, *103*, 166−170.

(23) Sastry, G. N.; Bally, T.; Hrouda, V.; Cársky, P. *J. Am. Chem. Soc.* **1998**, *120*, 9323−9334.

(24) Herbertz, T.; Roth, H. D. *J. Am. Chem. Soc.* **1998**, *120*, 11904−11911.

(25) Um, J. M.; Gutierrez, O.; Schoenebeck, F.; Houk, K. N.; MacMillan, D. W. C. *J. Am. Chem. Soc.* **2010**, *132*, 6001−6005.

(26) Bally, T.; Borden, W. T. In *Reviews in Computational Chemistry*; Lipkowitz, K. B., Boyd, D. B., Eds.; John Wiley and Sons, Inc.: New York, 1999; Vol. *13*, pp 1−97.

(27) Bally, T.; Sastry, G. N. *J. Phys. Chem. A* **1997**, *101*, 7923−7925.

(28) Braïda, B.; Hiberty, P. C. *J. Phys. Chem. A* **1998**, *102*, 7872−7877.

(29) (a) Zhao, Y.; Truhlar, D. G. *J. Chem. Phys.* **2006**, *125*, 194101. (b) Zhao, Y.; Truhlar, D. G. *J. Phys. Chem. A* **2006**, *110*, 13126−13130. (c) Zhao, Y.; Truhlar, D. G. *Theor. Chem. Acc.* **2008**, *120*, 215−241. (d) Zhao, Y.; Truhlar, D. G. *Acc. Chem. Res.* **2008**, *41*, 157−167.

(30) Zipse, H. *J. Am. Chem. Soc.* **1995**, *117*, 11798−11806.

(31) Oyama, M.; Nozaki, K. N.; Nagaoka, T.; Okazaki, S. *Bull. Chem. Soc. Jpn.* **1990**, *63*, 33−41.

(32) Mangion, D.; Arnold, D. R. *Acc. Chem. Res.* **2002**, *35*, 297−304.